4.7

MODELING AND VALIDATING THE DAILY ONSET OF THE FLORIDA EAST COAST SEA BREEZE OVER THE KENNEDY SPACE CENTER

Jonathan L. Case* and David A. Short
NASA Kennedy Space Center / Applied Meteorology Unit / ENSCO, Inc.

1. INTRODUCTION

The Canaveral Peninsula is the primary geographic feature of Florida's sub-tropical east coast, protruding some 30 km eastward from the mainland while sheltering Merritt Island and a complex of lagoons and islets from the Atlantic Ocean. Figure 1 shows the notable geographic features of the Canaveral Peninsula, including the Indian River, Banana River and Mosquito lagoon, the barrier island complex, Merritt Island, and the Florida mainland. The area is home to the Kennedy Space Center (KSC), Cape Canaveral Air Force Station (CCAFS), the KSC/CCAFS space launch complexes, the Merritt Island National Wildlife Refuge, and the Canaveral National Seashore.

A dominant meteorological feature in east-central Florida is the sea breeze. It is a mesoscale atmospheric circulation pattern, with a horizontal scale of tens to hundreds of kilometers, driven diurnally by differential heating between land and ocean (Atkinson 1981). The daily onset time and inland penetration distance of the sea-breeze front depends on the thermal contrast between land and water, and the large-scale atmospheric pressure gradient. The front typically migrates inland at a rate of 5 to 10 km h^{-1} (Wakimoto and Atkins 1994), causing rapid changes in wind speed, wind direction and relative humidity as it passes. Coastline configuration plays a role in the onset and propagation characteristics of the sea breeze with the complex configuration leading to intricate propagation characteristics. Differential heating also generates river/lagoon breezes along the inland waters, although their spatial scales tend be more localized, on the order of 1 to 10 km.

Wind speed and direction changes associated with the sea breeze affect the daily rhythms of life around Cape Canaveral, including those of natural ecosystems and those associated with human activities. For example, the sea breeze has the potential for influencing beach morphology and surf-zone hydrodynamics by wind stress effects on waves (Masselink and Pattiaratchi 1998). The sea-breeze front serves as a focusing mechanism for atmospheric convection, frequently triggering thunderstorms with heavy rain and lightning during the Florida summer months (López and Holle 1987). The wind field associated with the sea-breeze circulation also affects the potential transport of airborne pollutants and their dispersion, of special concern to space-launch operations. Due to these significant impacts of the sea-breeze front across east-central Florida, it is critically important to skillfully predict its occurrence, onset, and propagation rate in east-central Florida.

One of the tools available to weather forecasters to assist in sea-breeze prediction at CCAFS is real-time numerical weather prediction (NWP) output from a high-resolution configuration of the Regional Atmospheric Modeling System (RAMS). RAMS is run within the Eastern Range Dispersion Assessment System (ERDAS) to provide emergency response guidance for operations at KSC and CCAFS, in the event of an accidental hazardous material release or an aborted vehicle launch. The prognostic data from RAMS is available to ERDAS for display and input to the Hybrid Particle and Concentration Transport (HYPACT) dispersion model. The HYPACT model provides three-dimensional dispersion predictions using RAMS forecast grids. Because the wind field changes sharply along the sea-breeze front, the accuracy of the HYPACT dispersion predictions is highly dependent upon the accuracy of wind forecasts in RAMS. As a result, RAMS was designed to run at a sufficiently fine grid spacing in order to resolve adequately the evolution of the sea breeze and its interactions with local river and lagoon breezes.

This paper presents a comprehensive evaluation of daily RAMS sea-breeze forecasts across KSC/CCAFS during the 1999 and 2000 Florida summer months. The remainder of this paper is organized as follows. Section 2 describes the operational configuration of RAMS within ERDAS. Section 3 explains the methodology used to verify the occurrence and timing of the sea-breeze front across KSC/CCAFS. Section 4 presents the results of the nine-month evaluation. Section 5 compares sea-breeze forecast accuracy between two different grid configurations of RAMS. Finally, Section 6 provides a summary of the paper.

2. OPERATIONAL RAMS CONFIGURATION

In ERDAS, the three-dimensional, non-hydrostatic mode of RAMS is run operationally on four nested grids with horizontal grid spacing of 60, 15, 5, and 1.25 km, respectively (Fig. 2). The lateral boundary conditions are nudged (Davies 1983) by 12–36-h forecasts from the National Centers for Environmental Prediction Eta NWP model that have been interpolated onto an 80-km grid. Output from the Eta model is available every 6 h for boundary conditions to RAMS. Two-way interactive boundary conditions are utilized on the inner three grids. The physical parameterization schemes used in RAMS include a cloud microphysics scheme following Cotton *et al.* (1982), a modified Kuo cumulus convection scheme (Tremback 1990), the Chen and Cotton (1988) radiation scheme, a Mellor and Yamada (1982) type turbulence closure, and an 11-layer soil-

**Corresponding author address*: Jonathan Case, ENSCO, Inc., 1980 N. Atlantic Ave., Suite 230, Cocoa Beach, FL 32931. Email: case.jonathan@ensco.com

vegetation model with fixed soil moisture as the initial condition (Tremback and Kessler 1985). The modified Kuo scheme is run on grids 1–3 whereas the 1.25-km grid 4 utilizes explicit convection. The mixed-phase cloud microphysics scheme is run on all four grids.

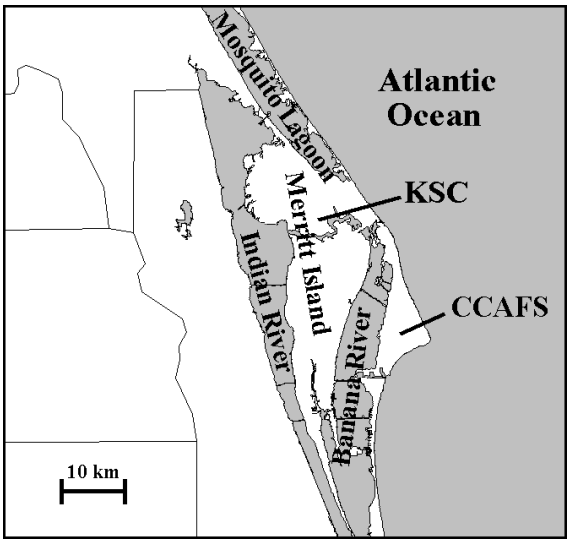

Figure 1. A plot of the geographical locations of the Kennedy Space Center (KSC), Cape Canaveral Air Force Station (CCAFS), and the local water bodies surrounding KSC/CCAFS.

Figure 2. The real-time RAMS domains for the 60-km mesh grid (grid 1) covering much of the southeastern United States and adjacent coastal waters, the 15-km mesh grid (grid 2) covering the Florida peninsula and adjacent coastal waters, the 5-km mesh grid (grid 3) covering east-central Florida and adjacent coastal waters, and the 1.25-km mesh grid (grid 4) covering the area immediately surrounding KSC/CCAFS.

RAMS is initialized twice-daily at 0000 and 1200 UTC using the Eta 12-h forecast grids and operationally-available observational data including the CCAFS rawinsonde, Aviation Routine Weather Reports, buoys, KSC/CCAFS wind-towers, and KSC/CCAFS 915-MHz and 50-MHz Doppler radar wind profiler data. No variational data assimilation or nudging technique is applied when incorporating observational data. Instead, RAMS is initialized from a cold start by integrating the model forward in time from a gridded field without any balancing or data assimilation steps. For the initial condition, observational data are analyzed onto hybrid coordinates using the RAMS isentropic analysis package (Tremback 1990). Details on the RAMS hardware configuration and run-time performance characteristics can be found in Case *et al.* (2000).

RAMS forecast output is available once per hour for display and analysis purposes. Thus, the sea-breeze verification study is limited in time to a frequency of one hour, regardless of the frequency of available observational data. Despite this limitation, hourly RAMS NWP output at high spatial resolution has the potential to provide valuable guidance for short-term forecasting of sea breezes in east-central Florida.

3. VERIFICATION METHODOLOGY

The sea-breeze verification was conducted at several individual KSC/CCAFS wind towers across east-central Florida. All archived RAMS forecasts from May–August 1999 and May–September 2000 were examined to verify the forecast sea breeze. Point forecasts were generated at each wind-tower site by interpolating in three dimensions the gridded RAMS forecasts from the innermost 1.25-km grid to the exact sensor height and location. These point forecasts and observations were examined at twelve selected KSC/CCAFS wind towers (Fig. 3), representing three different zones of east-central Florida (the coastal barrier islands, Merritt Island, and mainland Florida). In each zone, four towers were identified in a north-south orientation that contained the most data for both the 1999 and 2000 Florida warm seasons. Twelve-panel graphical plots displaying both the forecast and observed wind direction and speed were generated for all RAMS forecast cycles to verify the occurrence and timing of the sea breeze at each selected wind tower.

Both GOES-8 visible imagery and Weather Surveillance Radar, model 74C reflectivity data were used to identify the occurrence of the sea breeze on a given day. A sea-breeze front along Florida's east coast is typically accompanied by a sharp clearing line and reflectivity fine-line that propagate westward with time. To determine the occurrence and timing of the sea-breeze passage, each KSC/CCAFS wind tower was examined for the development and maintenance of a wind-shift to an onshore wind component (wind direction between 335° and 155°, the approximate orientation of the Florida coastline). The definition of an onshore versus offshore wind at coastal towers 1 and 3 varied from the rest of the towers due to the specific orientation of the coastline along the tip of Cape Canaveral (Fig. 3). At these towers, onshore flow was defined as a wind direction between 335° (NW) and

180° (S) at tower 1 and between 335° (NW) and 200° (SSW) at tower 3. As a result, both of these towers have a larger range of onshore wind directions compared to the other towers.

During easterly flow regimes, a sea-breeze passage was determined by a distinct increase in the negative (easterly) u-wind at each wind tower. These same wind criteria were then applied to the RAMS forecasts interpolated to each wind-tower location to determine the forecast sea-breeze passage. Finally, the occurrence of a forecast and observed sea breeze was verified on a per-tower basis in order to incorporate a spatial verification of the phenomenon on a given day. This methodology not only demands a high level of accuracy in the model predictions, but it also increases the size of the database.

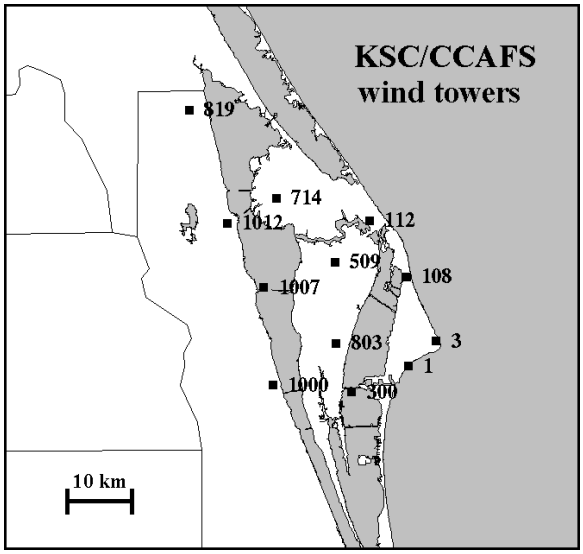

Figure 3. A plot of the 12 KSC/CCAFS wind towers used for the sea-breeze verification study.

A 2×2 contingency table was used to summarize the verification statistics based on the occurrence of both an observed and forecast sea breeze at any of the 12 KSC/CCAFS towers. A "hit" is defined as the occurrence of both an observed and forecast sea-breeze passage at a particular KSC/CCAFS tower. Because RAMS forecast output is available once per hour, the timing of the onset and movement of the sea-breeze front was verified to the nearest hour at each of the 12 KSC/CCAFS towers. Table 1 represents a sample 2×2 contingency table from which a variety of categorical and skill scores can be computed to measure forecast performance. The total number of correct forecasts is given by *x* in the upper left corner (forecast and observed = yes) and *w* in the lower right corner (forecast and observed = no). The number of forecast misses is given in the lower left portion of the table (forecast = no, observed = yes) and the number of false alarm forecasts is given in the upper right corner (forecast = yes, observed = no).

From the contingency table, a variety of categorical and skill scores can be calculated as defined in Schaefer (1990) and Doswell *et al.* (1990). These scores include the bias, Probability of Detection (POD), False Alarm Rate (FAR), Critical Success Index (CSI), and the Heidke Skill Score (HSS). Using the variables in Table 1, these scores are defined as follows:

TABLE 1. A sample 2×2 contingency table for the evaluation of a forecast element from which categorical and skill scores are computed (see text).

	Observed = Yes	*Observed = No*
Forecast = Yes	*x*	*z*
Forecast = No	*y*	*w*

Number of correct forecasts = (x+w)
Number of false alarm forecasts = z
Number of forecast misses = y

$$\text{Bias} = \frac{x+z}{x+y}, \tag{1}$$

$$\text{POD} = \frac{x}{x+y}, \tag{2}$$

$$\text{FAR} = \frac{z}{x+z}, \tag{3}$$

$$\text{CSI} = \frac{x}{x+y+z}, \tag{4}$$

$$\text{HSS} = \frac{2(xw-yz)}{y^2+z^2+2xw+(y+z)(x+w)}. \tag{5}$$

Given the occurrence of a weather element, the POD is the percentage of time that RAMS correctly forecasted that element. The FAR is the percentage of time that RAMS forecasted a weather element when none occurred. The CSI measures the ratio of the number of hits to the number of events plus the number of false alarms. The HSS provides a benchmark of the model performance compared to random forecasting (HSS=0). Higher POD, CSI, and HSS combined with a low FAR are associated with better performance of the model forecasts. In a perfect forecast, the bias, POD, CSI, and HSS are equal to 1 and the FAR is 0. The error statistics generated for the sea-breeze timing verification include root mean square (RMS) error and bias (in hours) in addition to the categorical and skill scores.

4. EVALUATION RESULTS

Tables 2 and 3 show a contingency table and categorical and skill scores for the occurrence of a sea-breeze passage at the 12 selected KSC/CCAFS towers during the 1999 and 2000 warm seasons. These tables represent nine months of data (May–August 1999 and May–September 2000) for both the 0000 and 1200 UTC RAMS forecast cycles. If no data were missing, the theoretical maximum number of elements in Table 2 would be 3312 for each forecast cycle (276 days multiplied by 12 wind towers); however, several

forecasts were missing and several towers experienced various outages, particularly during the 2000 warm season. In addition, when either the 0000 or 1200 UTC forecast was missing on a given day, the other forecast cycle was removed to maintain the exact same database for comparison between the two forecast cycles. As a result, about 75% (2469 elements) of the possible data are available for the overall sea-breeze evaluation.

Based on the results in Tables 2 and 3, observed sea-breeze passages occurred at the 12 wind towers about 65% of the time (1609 out of 2469 elements), of which RAMS correctly predicted 86% of them in the 0000 UTC cycle and 98% of them in the 1200 UTC cycle, according to the POD in Table 3. The probability of a null event (PON, not shown), the score analogous to POD for correct "no" forecasts of a sea breeze, indicates that both forecast cycles correctly predict non-sea breeze days only 66–70% of the time. The FAR is 16% for both the 0000 and 1200 UTC RAMS cycles. As a result of the higher POD in the 1200 UTC forecasts, this forecast cycle has the highest CSI and HSS. The HSS of 0.69 indicates that RAMS demonstrates a significant amount of utility in predicting the occurrence of the sea breeze. By applying statistical significance tests following the methodology used in Hamill (1999), each of the differences in scores between the 0000 and 1200 UTC forecasts were determined to be statistically significant at the 99% confidence level, except for the FAR.

TABLE 2. Contingency tables of the occurrence of the operational RAMS forecast versus observed sea breeze, verified at each of the 12 selected KSC/CCAFS towers of Figure 3 during the 1999 and 2000 Florida warm seasons.

0000 UTC Cycle	*Observed Sea Breeze*	*No Observed Sea Breeze*
Forecast Sea Breeze	1381	261
No Forecast Sea Breeze	228	599
1200 UTC Cycle	*Observed Sea Breeze*	*No Observed Sea Breeze*
Forecast Sea Breeze	1575	293
No Forecast Sea Breeze	34	567

In the instances when a correct yes forecast of a sea breeze occurred, the timing errors were determined at each of the wind towers during the 9-month evaluation period. Table 4 summarizes the timing error statistics for all the correct yes forecasts for both the 0000 and 1200 UTC cycles. In general, the RMS error ranges from 1.5–2.1 h for each category of wind towers. The errors are smallest at the coastal towers and largest at the mainland towers, but the variation between these locations is less than 0.5 h, which is smaller than the data-sampling rate of once per hour. In all instances the bias is -0.2 or -0.3 h, which is negligible compared to the sampling rate.

TABLE 3. Categorical and skill scores of RAMS forecast versus observed sea breezes during the 1999 and 2000 Florida warm seasons, associated with the contingencies in Table 2.

Parameter	*0000 UTC Cycle*	*1200 UTC Cycle*
POD	0.86	0.98
FAR	0.16	0.16
Bias	1.02	1.16
CSI	0.74	0.83
HSS	0.56	0.69

TABLE 4. A summary of timing error statistics for the May–August 1999 and May–September 2000 evaluation periods are given for the subjective sea-breeze verification performed for the 12 KSC/CCAFS tower locations of Figure 3. The RMS error and bias are shown in units of hours for the 0000 UTC and 1200 UTC forecast runs.

Location	**Statistic**	*0000 UTC Cycle*	*1200 UTC Cycle*
Coastal Towers	*RMS Error*	1.8	1.5
	Bias	-0.3	-0.3
Merritt Island Towers	*RMS Error*	1.9	1.7
	Bias	-0.3	-0.2
Mainland Towers	*RMS Error*	2.1	1.9
	Bias	-0.3	-0.2

5. GRID SPACING COMPARISON

In addition to the evaluation of the operational RAMS forecast sea breezes, a sensitivity test was conducted to compare the sea-breeze verification results between the operational RAMS and a coarser RAMS grid configuration during the 2000 warm season (May–September). This sensitivity experiment compared the RAMS 4-grid sea-breeze forecasts to RAMS 3-grid forecasts, where the innermost 1.25-km grid was simply excluded during the model's rerun of all forecasts during the 2000 warm season. As a result, the 3-grid RAMS configuration has a 5-km horizontal grid spacing over KSC/CCAFS. To generate point forecasts from the 3-grid RAMS, the gridded forecasts from the 5-km grid were interpolated to the sensor locations in the same manner as described in Section 3. The sea-breeze verification was then conducted at the

12 selected wind towers (Fig. 3) for all common 4-grid and 3-grid RAMS forecasts utilizing the same onshore versus offshore criteria at each wind tower.

According to Table 5, the 4-grid RAMS configuration outperforms the coarser 3-grid configuration in virtually all skill categories. The 0000 UTC POD is 11% higher in the 4-grid RAMS compared to the 3-grid configuration, resulting in an increase in both the CSI and HSS. In addition, the bias is very near unity in the 0000 UTC 4-grid runs whereas the 3-grid forecasts have a bias of 0.88 since it slightly under-forecasts the occurrence of the sea breeze (Table 5).

In the 1200 UTC RAMS forecasts, both model configurations improve in the categorical and skill scores except for the bias. The 4-grid forecasts continue to outperform the 3-grid forecasts in detecting the sea breeze over KSC/CCAFS. The POD improves to 98% in the 4-grid configuration and 92% in the 3-grid forecasts, whereas the CSI and HSS are 5% and 7% better, respectively, in the 4-grid versus 3-grid predictions (Table 5). All of the differences except the FAR are statistically significant above the 98% confidence interval [following the technique of Hamill (1999)], indicating that the 4-grid configuration is indeed a better forecaster of the sea-breeze occurrences compared to the coarser 3-grid RAMS configuration. The timing errors associated with the propagation of the sea-breeze front only experienced small differences between the 4-grid and 3-grid forecasts (not shown).

TABLE 5. Categorical and skill scores of the 0000 and 1200 UTC RAMS 4-grid and 3-grid forecast versus observed sea breezes during the 2000 Florida warm season.

	0000 UTC Forecast Cycle		**1200 UTC Forecast Cycle**	
Parameter	*RAMS 4-grid*	*RAMS 3-grid*	*RAMS 4-grid*	*RAMS 3-grid*
POD	0.82	0.71	0.98	0.92
FAR	0.17	0.19	0.15	0.15
Bias	0.98	0.88	1.15	1.08
CSI	0.70	0.61	0.84	0.79
HSS	0.54	0.41	0.71	0.64

Finally, Table 6 compares the skill between the 4-grid and 3-grid RAMS forecasts only at the mainland wind towers west of the Indian river. This group of wind towers exhibited the greatest discrepancy in skill between the 4-grid and 3-grid RAMS forecasts during the 2000 warm season. The POD is 14% higher in the 4-grid forecasts, resulting in a 9% higher CSI and 11% higher HSS. These results suggest that the 4-grid configuration better resolves the interactions between the river, lagoon, and sea breezes, providing an improvement in the low-level wind forecasts. The 5-km horizontal grid spacing of RAMS grid 3 is simply not sufficient to resolve river breeze circulations adequately since theoretically, it cannot resolve features whose wavelengths are less than 20 km (4 times the horizontal grid spacing). Meanwhile, the 1.25-km grid spacing can resolve features with wavelengths as small as 5 km, which is comparable to the scale of the river- and lagoon-breeze circulations. These results show that the higher resolution RAMS configuration had greater skill in predicting the sea breeze over the course of the 5-month 2000 warm season. The accurate prediction of phenomenological features such as the sea breeze are quite important in determining the added value of a modeling system for everyday forecasting at KSC/CCAFS.

TABLE 6. Categorical and skill scores of the combined 0000 and 1200 UTC RAMS sea-breeze forecasts from the 4-grid and 3-grid configurations during the 2000 Florida warm season, verified at only the four mainland KSC/CCAFS towers.

Parameter	**RAMS 4-grid**	**RAMS 3-grid**
POD	0.93	0.79
FAR	0.18	0.18
Bias	1.14	0.96
CSI	0.77	0.68
HSS	0.56	0.45

6. SUMMARY AND CONCLUSIONS

This paper presented the methodology and results for a comprehensive, nine-month verification of RAMS forecast sea-breezes over east-central Florida for the 1999 and 2000 Florida warm-season months. RAMS is run operationally at CCAFS to support weather forecasting and dispersion predictions during space launch operations. Based on the results presented in this paper, the operational RAMS configuration proved to be an excellent predictor of the occurrence of the sea breeze across KSC/CCAFS. The 1200 UTC forecast cycle outperformed the 0000 UTC cycle, but both forecast cycles exhibited significant skill (0.56 HSS in 0000 UTC, 0.69 HSS in 1200 UTC forecasts). The timing RMS errors associated with the forecast onset of the sea-breeze were between 1.5 and 2.1 hours at the 12 selected KSC/CCAFS wind towers and only a negligible timing bias occurred, relative to the hourly sampling rate of the data.

By comparing the operational RAMS 4-grid configuration (1.25 km inner grid spacing) to a coarser 3-grid configuration (5 km inner grid spacing), the 4-grid RAMS was found to be significantly better than the 3-grid design for both the 0000 and 1200 UTC forecast cycles. The most notable improvement occurred in the mainland KSC/CCAFS wind towers, suggesting that the finer grid spacing of the 4-grid configuration has a better handle of the interactions between the sea, river, and lagoon breezes. The accurate prediction of phenomenological features are quite important in determining the added value of a modeling system such

as RAMS for everyday forecasting and operational support at KSC/CCAFS.

7. REFERENCES

Atkinson, B. W., 1981: Meso-scale Atmospheric Circulations. Academic Press, 495 pp.

Case, J. L., J. Manobianco, A. V. Dianic, D. E. Harms, and P. N. Rosati, 2000: A sensitivity and benchmark study of RAMS in the Eastern Range Dispersion Assessment System. Preprints, *9th Conf. on Aviation, Range, and Aerospace Meteorology*, 11-15 September 2000, Orlando, FL, Amer. Meteor. Soc., 426-431.

Chen, S., and W. R. Cotton, 1988: The sensitivity of a simulated extratropical mesoscale convective system to longwave radiation and ice-phase microphysics. *J. Atmos. Sci.*, **45**, 3897-3910.

Cotton, W. R., M. A. Stephens, T. Nehrkorn, and G. J. Tripoli, 1982: The Colorado State University three-dimensional cloud/mesoscale model — 1982. Part II: An ice phase parameterization. *J. de Rech. Atmos.*, **16**, 295-320.

Davies, H. C., 1983: Limitations of some common lateral boundary schemes used in regional NWP models. *Mon. Wea. Rev.*, **111**, 1002-1012.

Doswell, C. A., R. Davies-Jones, and D. Keller, 1990: On summary measures of skill in rare event forecasting based on contingency tables. *Wea. Forecasting*, **5**, 576-585.

Hamill, T. M., 1999: Hypothesis tests for evaluating numerical precipitation forecasts. *Wea. Forecasting*, **14**, 155-167.

López, R. E., and R. L. Holle, 1987: Distribution of summertime lightning as a function of low-level wind flow in central Florida. Technical Memorandum, NOAA Environmental Research Labs, Boulder, CO, 43 p.

Masselink, G., and C. Pattiaratchi, 1998: The effect of sea breeze on beach morphology, surf zone, hydrodynamics and sediment resuspension. *Marine Geology*, **146**, 115-135.

Mellor, G. L., and T. Yamada, 1982: Development of a turbulence closure model for geophysical fluid problems. *Rev. Geophys. Space Phys.*, **20**, 851-875.

Schaefer, J. T., 1990: The critical success index as an indicator of warning skill. *Wea. Forecasting*, **5**, 570-575.

Tremback, C. J., 1990: Numerical simulation of a mesoscale convective complex: model development and numerical results. Ph.D. Dissertation, Atmos. Sci. Paper No. 465, Department of Atmospheric Science, Colorado State University, Fort Collins, CO 80523, 247 pp.

Tremback, C. J., and R. Kessler, 1985: A surface temperature and moisture parameterization for use in mesoscale numerical models. Preprints, *7th AMS Conf. on Numerical Weather Prediction*, June 17-20, Montreal, Quebec, Amer. Meteor. Soc., Boston, MA, 355-358.

Wakimoto, R.M., and N.T. Atkins, 1994: Observations of the sea-breeze front during CaPE. Part I: Single-Doppler, satellite, and cloud photogrammetric analysis. *Mon. Wea. Rev.*, **122**, 1092-1114.